

## Same-day imaging using small proteins: Clinical experience and translational prospects in oncology

Running title: Small Proteins for Radionuclide Imaging

Ahmet Krasniqi<sup>1</sup>, Matthias D'Huyvetter<sup>1</sup>, Nick Devoogdt<sup>1</sup>, Fredrik Y Frejd<sup>2,3</sup>, Jens Sörensen<sup>4,5</sup>, Anna Orlova<sup>6</sup>, Marleen Keyaerts<sup>1,7\*</sup>, Vladimir Tolmachev<sup>3\*</sup>

**\* Authors contributed equally**

<sup>1</sup>In Vivo Cellular and Molecular Imaging Laboratory (ICMI), VUB, Laarbeeklaan 103, B-1090 Brussels;  
<sup>2</sup>Affibody AB, Solna, Sweden; <sup>3</sup>Department of Immunology, Genetics and Pathology, Uppsala University, Uppsala, Sweden; <sup>4</sup>Nuclear Medicine and PET, Department of Surgical Sciences, Uppsala University, Uppsala, Sweden; <sup>5</sup>Medical Imaging Centre, Uppsala University Hospital, Uppsala, Sweden; <sup>6</sup>Department of Medicinal Chemistry, Uppsala University, Uppsala, Sweden. <sup>7</sup>Nuclear Medicine Department, UZ Brussel, Laarbeeklaan 101, B-1090 Brussels;

Corresponding author: Marleen Keyaerts, ICMI, VUB, Laarbeeklaan 103, B-1090 Brussels, 0032-2-477-50-20, [marleen.keyaerts@vub.ac.be](mailto:marleen.keyaerts@vub.ac.be)

First author: Ahmet Krasniqi (PhD candidate), ICMI, VUB, Laarbeeklaan 103, B-1090 Brussels, 0032-2-477-49-91, [ahmet.krasniqi@vub.be](mailto:ahmet.krasniqi@vub.be)

Word count: 5128

Financial support: AK has a doctoral grant from Agentschap Innoveren&Ondernemen (IWT.141388); MK is Senior Clinical Investigator and MD postdoctoral fellow of the Research Foundation – Flanders (FWO). Research was funded by CancerPlan Action (Federal Public Service Health, Food Chain Safety and Environment, Belgium), Kom-op-tegen-Kanker, FWO, Swedish Cancer Society and Swedish Research Council.

## **ABSTRACT**

Imaging of expression of therapeutic targets may enable patients' stratification for targeted treatments. The use of small radiolabeled probes based on the heavy-chain variable region of heavy-chain-only immunoglobulins or non-immunoglobulin scaffolds permits rapid localization of radiotracers in tumors and rapid clearance from normal tissues. This makes high-contrast imaging possible on the day of injection. This mini-review focuses on small proteins for radionuclide-based imaging that would allow same-day imaging, with the emphasis on clinical applications and promising preclinical developments within the field of oncology.

**Key words:** scaffold proteins, affibody, nanobody, radionuclide molecular imaging

## INTRODUCTION

The discovery of key pathways that drive disease progression has led to the identification of new targetable molecules. When such molecules are located on the cell membrane or in the extracellular space, monoclonal antibodies (mAbs) can often block or activate these pathways. These mAbs typically show a slow systemic clearance, allowing a tri-weekly treatment regimen. Several mAbs have been used for Positron Emission Tomography (PET) imaging, the so-called immuno-PET approach (1). This approach allows studying the pharmacokinetics and receptor occupancy of the therapeutics, as well as the presence and accessibility of the molecular target in the individual patient. As these mAbs are produced in large quantities by pharma industry as therapeutics, they are typically available as targeting moiety for the development of an imaging agent at very low cost. A major disadvantage is the long blood circulation time, with half lives up to 28 days, requiring delayed scanning time points typically between 4 and 6 days (Fig. 1A). Even at that time, appreciable quantities of the tracer remain in the blood, resulting in low sensitivity due to high background and low specificity due to enhanced permeability and retention effect, especially for targets with a low expression level.

To overcome the slow clearance and extravasation, mAbs have been engineered to smaller fragments such as antigen-binding (Fab, Fab2), variable (Fv), and single-chain variable (scFv) fragments, diabodies and minibodies (2), with a molecular weight between 25 and 110 kDa. Although this size reduction increases the clearance rate of nonbound tracers, the clearance and extravasation rate remain overall too low to allow

same-day imaging with sufficient contrast. Attractive alternative targeting proteins, with further reduction in size, are Camelid single-domain Ab fragments (sdAb) and several non-immunoglobulin protein scaffolds such as affibody molecules, anticalins, designed ankyrin repeat proteins (DARPin) and fibronectin type III (FN3, adnectins) (Fig. 2, Table 1) (3). Their low molecular weight enable very fast penetration in tumor tissues and their lack of Fc-region further improves clearance. They allow a same-day imaging approach, much like the current practice for  $^{18}\text{F}$ -FDG-PET, and their application results in a 4-to-6-fold lower radiation exposure versus immuno-PET, making them attractive for routine use. This approach is very promising to assess target expression levels in individual patients in order to identify patients that will likely benefit from targeted treatments.

## GENERATION AND TYPICAL CHARACTERISTICS OF SMALL PROTEINS

SdAbs, also referred to as Nanobodies (tradename company Ablynx<sup>®</sup>), represent the smallest functional antibody fragments (12-15 kDa), consisting of the heavy-chain variable region of an immunoglobulin type that is naturally present in *Camelidae*. sdAbs are typically highly stable and bind antigens fast with high specificity and affinity. Due to their small size, sdAbs show improved tissue penetration compared to mAbs (4). For their generation, camelids are immunized with the antigen of choice. The sdAb gene fragments are amplified from isolated lymphocytes, providing a library of potential binders. Affinity-matured target-specific sdAbs are selected via protein display and biopanning and finally produced in microbial hosts.

Besides antibody fragments, which are derived from different types of antibody classes, also different scaffold-proteins have been engineered as small-sized imaging probes (5). Scaffold-proteins fall into two structural classes: (i) domain-sized compounds (6–20 kDa) like affibody molecules, ABD-derived affinity proteins (ADAPTs), affilins, anticalins, atrimers, DARPins, FN3 scaffolds, fynomers, kunitz domains or pronectins and (ii) constrained peptides (2–4 kDa) like vimers, bicyclic peptides and cystine knot peptides (3). For both types of scaffold-proteins, a library of potential binders is typically generated by random or targeted mutagenesis of the parent scaffold protein at residues that are not essential for protein folding. From this, target-specific binders are selected via phage display, yeast surface display or ribosome/mRNA display. Most sdAbs and engineered scaffold-proteins are easily produced in microbial systems, are stable and soluble and show good binding affinity and specificity (3). So far, several sdAbs and

scaffold-proteins, selected against different targets, have been used as probes for Single-photon Emission Computed Tomography (SPECT) and PET imaging (4,5).

## **SDABS IN RADIONUCLIDE IMAGING**

SdAbs have been successfully applied as probes for radionuclide imaging, of which the *human epidermal growth factor receptor* (HER2)-targeting sdAbs are most dominantly explored. HER2 is an interesting therapeutic target, as it is overexpressed in several cancers including breast, ovarian and gastric. The <sup>68</sup>Ga-labeled HER2-targeting sdAb “2Rs15d” enabled high contrast PET-imaging of HER2-positive breast cancer at 1h post injection (p.i.) in SKOV-3 xenografts (tumor-to-blood ratio of 29±8)(6). A GMP-grade version was evaluated in a phase I PET study in HER2-positive breast cancer patients (Fig. 1B). The compound was safe, with fast urinary clearance, resulting in a biological half-life of 1h and only 10% of injected activity remaining in the blood at 1h p.i. Biodistribution data showed background uptake in liver, kidneys and to a lesser extent in bowel and salivary glands. Uptake was high in both primary HER2-positive tumors and metastasis with mean uptake values up to 11.8 and 6.0 respectively at 1h p.i. (Fig. 1B). The effective dose was 0.043 mSv/MBq, resulting in an average of 4.6 mSv per patient, with the critical organ being the urinary bladder wall (0.406 mGy/MBq) (7). The same HER2-targeting sdAb was also <sup>18</sup>F-labeled and tested preclinically, with high tumor-to-blood ratio (13±2 as early as 1h p.i.). Uptake in kidneys was however only half of that measured for <sup>68</sup>Ga-labeled 2Rs15d (8) which could further decrease the radiation exposure. Finally, 2Rs15d was successfully radiolabeled with <sup>131</sup>I and showed superior

tumor uptake and remarkably low kidney retention in HER2-positive tumor xenografted mice. (9). Consequently, this version is now being evaluated as a theranostic drug in a first clinical breast cancer trial (NCT02683083). Another HER2-targeting sdAb, 5F7, was radiolabeled with both  $^{18}\text{F}$  and  $^{125}\text{I}$  and also demonstrated high-contrast imaging in preclinical studies (10-12).

A promising target is the *prostate-specific membrane antigen* (PSMA), as it is expressed on virtually all metastatic prostate cancers. A PSMA-targeted sdAb (PSMA30) radiolabeled with  $^{99\text{m}}\text{Tc}$  demonstrated fast and specific uptake in PSMA-positive xenografts (tumor-to-blood ratio of 8.7 at 90 min p.i.) (Fig. 3A, (13)). Another PSMA-targeting sdAb (JVZ-007) was labeled with  $^{111}\text{In}$  for SPECT/CT imaging. Excellent tumor targeting as early as 3h p.i. was observed (tumor-to-blood ratio of  $48\pm 5$ ), in the absence of nonspecific uptake (14). Given the current success of clinical imaging using the available PSMA-binding peptides, the question remains if these sdAbs have enough added value to bring them to the clinic.

*CD20* is expressed in over 90% of B-cell Non-Hodgkin lymphomas, and is clinically used for targeted radionuclide therapy with monoclonal antibodies ( $^{90}\text{Y}$ -ibritumomab; Zevalin<sup>®</sup>). Recently, Krasniqi et al. selected a lead CD20-targeting sdAb 9079 and confirmed its potential for same-day PET imaging in a preclinical model (tumor-to-blood ratio of approximately 4) (Fig. 3B, (15)).

Traditionally, targets selected for molecular imaging and therapy were those overexpressed on the tumor cells themselves. More recently, interest has raised in targets expressed on the tumor stroma since they can play important roles in tumor

angiogenesis, invasion and immune escape. Such targets are typically less abundantly present in the tumor, which demands a sensitive and very specific technique. It is expected that tracers with slow clearance will not be able to accurately discern such expression from remaining background signals, making the use of sdAb and scaffolds the ideal choice. A promising sdAb is one that targets the *macrophage mannose receptor (MMR)*. MMR is highly expressed on pro-tumorogenic tumor-associated macrophages that play an important role in tumor growth, tumor angiogenesis, metastasis and immune suppression. Being able to visualize and quantify the presence of MMR (and thus tumor-associated macrophages) in tumor tissue might be a helpful prognostic tool for the treatment of cancer. To this end, Movahedi and coworkers selected and preclinically validated a lead anti-MMR sdAb (Fig. 3A, (16)). A  $^{18}\text{F}$ -labeled variant was successfully developed as a PET tracer for MMR expression in mice (17), confirming its potential for clinical translation.

Other promising targets within tumor stroma are the immune checkpoints. Successes of immune checkpoint blockade with cytotoxic T-lymphocyte-associated protein-4 and *PD-1/PD-L1 (Programmed Death (Ligand) 1)* antibody therapy are however only seen in a subset of all cancer patients. Biomarker imaging might help to select patients for such therapies. Anti-PD-L1 sdAbs were developed that could allow the assessment of PD-L1 expression in the tumor micro-environment (Fig. 3A) (18,19).

## **AFFIBODY MOLECULES IN RADIONUCLIDE IMAGING**



HER2-targeting affibody molecules were the first scaffold proteins evaluated for radionuclide molecular imaging. The second generation affibody molecules ABY-025 labeled with  $^{111}\text{In}$  for SPECT and  $^{68}\text{Ga}$  for PET imaging were evaluated in Phase I/II clinical studies for assessment of HER2-expression in breast cancer metastases (Fig. 1C) (20,21). ABY-025 was found to be safe in humans, and no anti-affibody antibodies were found after repeated administration. The effective radiation doses were  $0.15\pm 0.02$  mSv/MBq (21 mSv/patient) for  $^{111}\text{In}$  and  $0.028\pm 0.003$  mSv/MBq (5.6 mSv/patient) for  $^{68}\text{Ga}$  (20,22). Injection of 500  $\mu\text{g}$  of  $^{68}\text{Ga}$ -ABY-025 provided better sensitivity and specificity than 100  $\mu\text{g}$ , mainly because of reduced retention in the liver (21). Comparison with immunohistochemical staining of biopsy material demonstrated that the measurement of the maximal uptake value 2-4h p.i. permits clear discrimination between metastases with 3+ and 2+ levels of HER2-expression (21). Furthermore, spleen can be used as an intra-image reference tissue to calculate tumor-to-spleen ratios, permitting a simple and robust discrimination between metastases with high and low HER2-expression using both PET and SPECT (23), which makes the diagnosis independent of external hardware calibrations.

High renal reabsorption of affibody molecules complicates their use for radionuclide therapy. However, internalization of anti-HER2 affibody molecules is slow after binding to malignant cells but rapid in proximal tubuli. The peptide-based chelator GGGC provides non-residualizing  $^{188}\text{Re}$ -labeling, thereby resulting in good tumor retention but rapid washout from kidneys (24). Extrapolation to humans suggests that the absorbed dose to tumors would exceed the kidney approximately 3.4-fold. An

alternative might be an affibody-based pretargeting. Two approaches were evaluated: one mediated by a bioorthogonal reaction between trans-cyclooctene and tetrazine (25) and another mediated by an interaction between two complementary peptide nucleic acids (26). Both methodologies provided appreciably higher uptake of radiometals in tumors than in kidneys, with the peptide nucleic acids-mediated approach resulting in better tumor retention.

Resistance to trastuzumab therapy may be associated with overexpression of *human epidermal growth factor type 3 (HER3)* and *insulin-like growth factor type 1 receptor (IGF-1R)* (27). Imaging of an emerging expression of these receptors might suggest an onset of resistance and a need to modify treatment. Expression of these receptors is also essential in other malignancies (e.g. prostate and ovarian carcinomas), and multiple therapeutics targeting HER3/IGF-1R are under development. A challenge in imaging of both receptors is a modest expression level in malignant cells (typically below 40000 receptors/cell) and its expression in normal tissues. Affibody molecules were selected for both molecular targets. To mimic the clinical situation, binders with approximately equal affinity to human and murine receptors were generated. An anti-IGF-1R affibody molecule ZIGF1R:4551 was labeled using [ $^{99m}\text{Tc}(\text{CO})_3$ ] and demonstrated receptor-specific uptake in both IGF-1R expression tumors and tissues (28) (Fig. 4A). An anti-HER3 affibody molecule Z08698 with affinity of 50 pM was labeled earlier with  $^{111}\text{In}$  and  $^{99m}\text{Tc}$  for SPECT imaging. To enable straightforward quantification, the HEHEHE-Z08698-NOTA was labeled with positron-emitting  $^{68}\text{Ga}$ , showing accumulation in tumor xenografts that was proportional to HER3-expression level (Fig. 4B) (29).

*Epidermal growth factor receptor (EGFR)* is the molecular target for several mAbs and tyrosine kinase inhibitors. Detection of overexpression may help to predict outcomes for some treatment regimens of non-small cell lung cancer and head-and-neck squamous cell carcinoma. One of the challenges in imaging EGFR expression is its expression in liver and some other tissues. ZEGFR:2377 having equal affinity to murine and human EGFR ( $K_D$  of 0.8-0.9 nM) was selected and an injection of 30-50  $\mu$ g partially saturates receptors in healthy tissues but not in tumors. Labelling of DOTA-ZEGFR:2377 with  $^{68}\text{Ga}$  and  $^{57/55}\text{Co}$  was assessed. Evaluation of conjugates in A431 xenografts demonstrated that radiocobalt-labeled ZEGFR:2377 provides significantly higher tumor-to-organ ratios than gallium-labeled (43). Importantly, a tumor-to-liver ratio of  $3.1 \pm 0.5$  (3h p.i.) was obtained (Fig. 4A).

*Carbonic anhydrase IX (CAIX)* is overexpressed by hypoxic cells, and imaging of CAIX expression may be utilized for identification of radioresistant hypoxic tumors. In addition, CAIX is expressed by normoxic renal cell carcinoma and may be used to distinguish between malignant and benign renal tumors. A panel of anti-CAIX affibody molecules labeled with  $^{99\text{m}}\text{Tc}$  and  $^{125}\text{I}$  was evaluated in SK-RC-52 renal cell carcinoma (30). The best hypoxia tracer was  $^{99\text{m}}\text{Tc}-(\text{HE})_3\text{-ZCAIX:2}$ .  $^{125}\text{I}\text{-ZCAIX:4}$  was best suited for imaging of renal cell carcinoma with tumor-to-kidney ratio of  $2.1 \pm 0.5$  (Fig. 4A).

Inhibition of *platelet-derived growth factor receptor beta (PDGFR $\beta$ )* in tumor stroma (pericytes of neovasculature and cancer associated fibroblasts) normalizes tumor interstitial pressure and improves drug uptake and efficacy. An anti-PDGFR $\beta$  affibody molecule DOTA-Z09591 was labeled with  $^{68}\text{Ga}$  and evaluated as a potential

companion diagnostics (31). In mice,  $^{68}\text{Ga}$ -DOTA-Z09591 provided clear visualization of U-87 MG xenografts (36000 PDGFR $\beta$  receptors/cell) at 2h p.i. (Fig. 4B).

To evaluate *PD-L1* expression before PD-1/PD-L1-targeting therapy and for response monitoring, a *PD-L1*-specific affibody molecule with  $K_D$  of 1 nM was selected (32). This NOTA-conjugated  $Z_{\text{PD-L1}_1}$  was labeled with  $^{18}\text{F}$  using  $^{18}\text{F}$ -AIF.  $^{18}\text{F}$ -AIF-NOTA- $Z_{\text{PD-L1}_1}$  enabled specific imaging of PD-L1 in murine models, with tumor-to-blood ratio exceeding values obtained using radiolabeled antibodies several days after injection (Fig. 4B).

## PRECLINICAL STUDIES WITH OTHER PROTEIN-SCAFFOLDS

### Knottins

Inhibitor cystine-knots, also known as knottin-peptides, are small polypeptides consisting of 30-50 amino acids with a molecular weight of about 4 kDa. They are characterized by their structural motif with 3 cystine bridges, forming a knot, and can be found in a wide range of animals, plants and fungi (3).

Kimura et al. reported a knottin-peptide that binds to  $\alpha_v\beta_6$ , an integrin overexpressed in many cancers. It demonstrated fast and specific tumor targeting in mice bearing  $\alpha_v\beta_6$ -expressing tumors. However, low tumor-to-liver, tumor-to-kidney, tumor-to-gut ratios were also observed (33).

Jiang et al. reported the potential use of a 7C knottin-peptide as a SPECT probe for imaging of integrin  $\alpha_v\beta_3$  positive tumors. Despite the fact that no SPECT imaging data were shown, biodistribution study in mice revealed fast and specific accumulation of

$^{111}\text{In}$ -labeled 7C in  $\alpha_v\beta_3$ -positive human subcutaneously growing U87MG glioblastoma at 0.5h p.i. (34).

More recently, the  $^{18}\text{F}$ -labeled divalent integrin  $\alpha_v\beta_3$ -targeting knottin-peptide 3-4A, containing two separate integrin-binding paratopes, was evaluated in subcutaneously growing U87MG xenografts (35). Images revealed clear uptake in tumors after 30 min, with low background signal, except in kidneys (Fig. 5B).

### **DARPin**

Designed ankyrin repeat proteins (DARPin) are scaffold-proteins with a size of 14-18 kDa, which are derived from natural ankyrin repeat (AR) proteins. Synthetic DARPin libraries have been designed to select DARPins against different targets, mainly for non-radioactive therapeutic applications (3).

Goldstein et al. described SPECT-imaging of HER2 expression using  $^{125}\text{I}$ -/ $^{111}\text{In}$ -labeled G3 DARPin (Fig. 5A). High tumor uptake was measured for both isotopes in mice bearing human BT474 HER2-positive xenografts at 4h p.i. However, the lower uptake of  $^{111}\text{In}$ -compound in normal tissues led to higher tumor-to-background ratios compared to its  $^{125}\text{I}$  counterpart (36).

### **FN3 - Adnectin Scaffolds**

A small anti-CD20 receptor protein has been generated, based on the 10 kDa human FN3, for PET imaging of B-cell lymphomas (37).  $^{64}\text{Cu}$ -DOTA-FN3<sub>CD20</sub> was evaluated in human CD20-transgenic mice, showing a high specific accumulation in the spleen and other CD20-expressing organs, already at 1h p.i.. In non-transgenic mice

bearing human CD20 tumors,  $^{64}\text{Cu}$ -FN3<sub>CD20</sub> showed specific tumor targeting with low healthy tissue uptake as early as 4h p.i. (37).

Recently, synthesis of human and cynomolgus crossreactive anti-PD-L1 FN3-scaffold was described. *In vivo* PET imaging with  $^{18}\text{F}$ -labeled scaffold ( $^{18}\text{F}$ -BMS-986192) clearly visualized PD-L1 tumors in mice at 2h p.i. (Fig. 5B) (38). Cynomolgus PET imaging showed specific binding of  $^{18}\text{F}$ -BMS-986192 in the spleen, with a fast blood clearance through kidneys and bladder. Currently, this compound is tested in a single-center substudy of the CheckMate 511 clinical trial (NCT02714218/EudraCT 2015-004920-67), to evaluate its potential as biomarker in metastatic melanoma patients (38).

## ADAPTs

ADAPTs utilize a 46-amino-acid scaffold of an albumin-binding domain (5.2 kDa) of streptococcal protein G. The anti-HER2 ADAPT6 was selected for its high affinity binding (1.1 nM), and its loss of binding to albumin to facilitate fast blood clearance. ADAPT6 was site-specifically DOTA-conjugated at the N-terminus (39).  $^{111}\text{In}$ -DOTA-ADAPT6 showed high uptake in SKOV-3 xenografts and tumor-to-blood ratio already at 1h p.i.  $^{68}\text{Ga}$ -DOTA-ADAPT6-PET enabled clear discrimination between xenografts with high and low expression. Re-absorption of ADAPT6 in kidneys was high, and could not be reduced using injection of cationic amino acids or Gelofusine. Further studies demonstrated that targeting properties of ADAPTs might be appreciably improved by modification of labeling chemistry and N-terminus composition. An optimized  $^{111}\text{In}$ -labeled variant DOTA-Cys<sup>59</sup>-ADAPT6 had a tumor-to-blood ratio of  $277\pm 35$  at 4h p.i. The use of non-residualizing  $^{125}\text{I}$ -HPEM label provided tumor-to-kidney ratio of  $13\pm 3$ , which opens a way for radionuclide therapy (Fig. 5A) (40).

It has to be noted that the radiolabeling chemistry might influence properties of targeting proteins by modification of critical amino acids and/or local charge and lipophilicity on the protein surface. This might affect on-target and off-target interactions, excretion and intracellular retention of the radionuclide after internalization (41). In this way, changes in radiolabeling chemistry might have important effects on the imaging contrast obtained and optimal imaging time point. Therefore, a meticulous optimization of labeling chemistry is crucial for high-sensitivity imaging using small proteins.

## **CONCLUSIONS**

sdAbs and affibody proteins have clinically confirmed the safety, low radiation exposure and high potential for molecular imaging in cancer patients. Although studies with larger patient cohorts are required to establish their exact clinical value, the early-phase data for HER2-specific probes are very encouraging. Also a number of emerging sdAb- and scaffold protein-based probes that target other clinically relevant targets have been developed preclinically and their clinical translation could impact patient care in the future.



## **DISCLOSURE**

MK has received travel and accommodation expenses from Bayer NV; ND and MD are co-founders of CamelIDs. ND has received funding from Boehringer-Ingelheim, Complix. AK, MK, ND and MD have patents on Nanobody imaging and therapy. FYF is an employee of Affibody AB, FYF, AO and VT have patents on Affibody development and applications.

## **ACKNOWLEDGMENTS:**

AK is a doctoral fellow from Agentschap Innoveren&Ondernemen (IWT.141388); MK is Senior Clinical Investigator and MD postdoctoral fellow of the Research Foundation–Flanders (FWO). Research was funded by CancerPlan Action (Federal Public Service Health, Food Chain Safety and Environment, Belgium), Kom-op-tegen-Kanker, FWO, Swedish Cancer Society and Swedish Research Council.

## REFERENCES

1. Lamberts LE, Williams SP, Terwisscha van Scheltinga AG, et al. Antibody positron emission tomography imaging in anticancer drug development. *J Clin Oncol*. 2015;33:1491-1504.
2. Hudson PJ, Souriau C. Engineered antibodies. *Nat Med*. 2003;9:129-134.
3. Simeon R, Chen Z. In vitro-engineered non-antibody protein therapeutics. *Protein Cell*. 2017;doi: 10.1007/s13238-017-0386-6.
4. De Vos J, Devoogdt N, Lahoutte T, Muyltermans S. Camelid single-domain antibody-fragment engineering for (pre)clinical in vivo molecular imaging applications: adjusting the bullet to its target. *Expert Opin Biol Ther*. 2013;13:1149-1160.
5. Miao Z, Levi J, Cheng Z. Protein scaffold-based molecular probes for cancer molecular imaging. *Amino Acids*. 2011;41:1037-1047.
6. Xavier C, Vaneycken I, D'Huyvetter M, et al. Synthesis, preclinical validation, dosimetry, and toxicity of <sup>68</sup>Ga-NOTA-anti-HER2 Nanobodies for iPET imaging of HER2 receptor expression in cancer. *J Nucl Med*. 2013;54:776-784.
7. Keyaerts M, Xavier C, Heemskerk J, et al. Phase I study of <sup>68</sup>Ga-HER2-Nanobody for PET/CT assessment of HER2 expression in breast carcinoma. *J Nucl Med*. 2016;57:27-33.
8. Xavier C, Blykers A, Vaneycken I, et al. (18)F-nanobody for PET imaging of HER2 overexpressing tumors. *Nucl Med Biol*. 2016;43:247-252.
9. D'Huyvetter M, De Vos J, Xavier C, et al. <sup>131</sup>I-labeled anti-HER2 camelid sdAb as a theranostic tool in cancer treatment. *Clin Cancer Res*. 2017;23(21):6616-6628.
10. Vaidyanathan G, McDougald D, Choi J, et al. Preclinical evaluation of <sup>18</sup>F-labeled anti-HER2 Nanobody conjugates for imaging HER2 receptor expression by immuno-PET. *J Nucl Med*. 2016;57:967-973.
11. Pruszynski M, Koumarianou E, Vaidyanathan G, et al. Targeting breast carcinoma with radioiodinated anti-HER2 Nanobody. *Nucl Med Biol*. 2013;40:52-59.
12. Pruszynski M, Koumarianou E, Vaidyanathan G, et al. Improved tumor targeting of anti-HER2 nanobody through N-succinimidyl 4-guanidinomethyl-3-iodobenzoate radiolabeling. *J Nucl Med*. 2014;55:650-656.

- 13.** Evazalipour M, D'Huyvetter M, Tehrani BS, et al. Generation and characterization of nanobodies targeting PSMA for molecular imaging of prostate cancer. *Contrast Media Mol Imaging*. 2014;9:211-220.
- 14.** Chatalic KL, Veldhoven-Zweistra J, Bolkestein M, et al. A novel (1)(1)(1)In-labeled anti-prostate-specific membrane antigen Nanobody for targeted SPECT/CT imaging of prostate cancer. *J Nucl Med*. 2015;56:1094-1099.
- 15.** Krasniqi A, D'Huyvetter M, Xavier C, et al. Theranostic radiolabeled anti-CD20 sdAb for targeted radionuclide therapy of Non-Hodgkin Lymphoma. *Mol Cancer Ther*. 2017;DOI 10.1158/1535-7163.MCT-17-0554.
- 16.** Movahedi K, Schoonooghe S, Laoui D, et al. Nanobody-based targeting of the macrophage mannose receptor for effective in vivo imaging of tumor-associated macrophages. *Cancer Res*. 2012;72:4165-4177.
- 17.** Blykers A, Schoonooghe S, Xavier C, et al. PET imaging of macrophage mannose receptor-expressing macrophages in tumor stroma using <sup>18</sup>F-radiolabeled Camelid single-domain antibody fragments. *J Nucl Med*. 2015;56:1265-1271.
- 18.** Broos K, Keyaerts M, Lecocq Q, et al. Non-invasive assessment of murine PD-L1 levels in syngeneic tumor models by nuclear imaging with nanobody tracers. *Oncotarget*. 2017;8:41932-41946.
- 19.** Ingram JR, Dougan M, Rashidian M, et al. PD-L1 is an activation-independent marker of brown adipocytes. *Nat Commun*. 2017;8:647.
- 20.** Sorensen J, Sandberg D, Sandstrom M, et al. First-in-human molecular imaging of HER2 expression in breast cancer metastases using the <sup>111</sup>In-ABY-025 affibody molecule. *J Nucl Med*. 2014;55:730-735.
- 21.** Sorensen J, Velikyan I, Sandberg D, et al. Measuring HER2-receptor expression in metastatic breast cancer using [<sup>68</sup>Ga]ABY-025 Affibody PET/CT. *Theranostics*. 2016;6:262-271.
- 22.** Sandstrom M, Lindskog K, Velikyan I, et al. Biodistribution and radiation dosimetry of the anti-HER2 Affibody molecule <sup>68</sup>Ga-ABY-025 in breast cancer patients. *J Nucl Med*. 2016;57:867-871.
- 23.** Sandberg D, Tolmachev V, Velikyan I, et al. Intra-image referencing for simplified assessment of HER2-expression in breast cancer metastases using the Affibody molecule ABY-025 with PET and SPECT. *Eur J Nucl Med Mol Imaging*. 2017;44:1337-1346.

24. Altai M, Wallberg H, Honarvar H, et al.  $^{188}\text{Re}$ -ZHER2:V2, a promising affibody-based targeting agent against HER2-expressing tumors: preclinical assessment. *J Nucl Med*. 2014;55:1842-1848.
25. Altai M, Perols A, Tsourma M, et al. Feasibility of Affibody-based bioorthogonal chemistry-mediated radionuclide pretargeting. *J Nucl Med*. 2016;57:431-436.
26. Honarvar H, Westerlund K, Altai M, et al. Feasibility of Affibody molecule-based PNA-mediated radionuclide pretargeting of malignant tumors. *Theranostics*. 2016;6:93-103.
27. Nahta R, Yu D, Hung MC, Hortobagyi GN, Esteva FJ. Mechanisms of disease: understanding resistance to HER2-targeted therapy in human breast cancer. *Nat Clin Pract Oncol*. 2006;3:269-280.
28. Orlova A, Hofstrom C, Strand J, et al.  $^{99m}\text{Tc}(\text{CO})_3^+-(\text{HE})_3\text{-ZIGF1R:4551}$ , a new Affibody conjugate for visualization of insulin-like growth factor-1 receptor expression in malignant tumours. *Eur J Nucl Med Mol Imaging*. 2013;40:439-449.
29. Rosestedt M, Andersson KG, Mitran B, et al. Affibody-mediated PET imaging of HER3 expression in malignant tumours. *Sci Rep*. 2015;5:15226.
30. Garousi J, Honarvar H, Andersson KG, et al. Comparative evaluation of Affibody molecules for radionuclide imaging of in vivo expression of carbonic anhydrase IX. *Mol Pharm*. 2016;13:3676-3687.
31. Strand J, Varasteh Z, Eriksson O, Abrahmsen L, Orlova A, Tolmachev V. Gallium-68-labeled affibody molecule for PET imaging of PDGFRbeta expression in vivo. *Mol Pharm*. 2014;11:3957-3964.
32. Gonzalez Trotter DE, Meng X, McQuade P, et al. In vivo imaging of the programmed death ligand 1 by  $^{18}\text{F}$  positron emission tomography. *J Nucl Med*. 2017;10.2967/jnumed.117.191718.
33. Kimura RH, Teed R, Hackel BJ, et al. Pharmacokinetically stabilized cystine knot peptides that bind alpha-v-beta-6 integrin with single-digit nanomolar affinities for detection of pancreatic cancer. *Clin Cancer Res*. 2012;18:839-849.
34. Jiang L, Miao Z, Kimura RH, et al.  $^{111}\text{In}$ -labeled cystine-knot peptides based on the Agouti-related protein for targeting tumor angiogenesis. *J Biomed Biotechnol*. 2012;2012:368075.
35. Jiang L, Kimura RH, Ma X, et al. A radiofluorinated divalent cystine knot peptide for tumor PET imaging. *Mol Pharm*. 2014;11:3885-3892.

- 36.** Goldstein R, Sosabowski J, Livanos M, et al. Development of the designed ankyrin repeat protein (DARPin) G3 for HER2 molecular imaging. *Eur J Nucl Med Mol Imaging*. 2015;42:288-301.
- 37.** Natarajan A, Hackel BJ, Gambhir SS. A novel engineered anti-CD20 tracer enables early time PET imaging in a humanized transgenic mouse model of B-cell non-Hodgkins lymphoma. *Clin Cancer Res*. 2013;19:6820-6829.
- 38.** Donnelly DJ, Smith RA, Morin P, et al. Synthesis and biological evaluation of a novel 18F-labeled Adnectin as a PET radioligand for imaging PD-L1 expression. *J Nucl Med*. 2017;10.2967/jnumed.117.199596.
- 39.** Garousi J, Lindbo S, Nilvebrant J, et al. ADAPT, a novel scaffold protein-based probe for radionuclide imaging of molecular targets that are expressed in disseminated cancers. *Cancer Res*. 2015;75:4364-4371.
- 40.** Lindbo S, Garousi J, Mitran B, et al. Radionuclide tumor targeting using ADAPT scaffold proteins: aspects of label positioning and residualizing properties of the label. *J Nucl Med*. 2018;Jan;59(1):93-99.
- 41.** Tolmachev V, Orlova A. Influence of labelling methods on biodistribution and imaging properties of radiolabelled peptides for visualisation of molecular therapeutic targets. *Curr Med Chem*. 2010;17:2636-2655.
- 42.** Dijkers EC, Oude Munnink TH, Kosterink JG, et al. Biodistribution of 89Zr-trastuzumab and PET imaging of HER2-positive lesions in patients with metastatic breast cancer. *Clin Pharmacol Ther*. 2010;87:586-592.
- 43.** Garousi J, Andersson KG, Dam JH, et al. The use of radiocobalt as a label improves imaging of EGFR using DOTA-conjugated Affibody molecule. *Sci Rep*. 2017;7:5961.

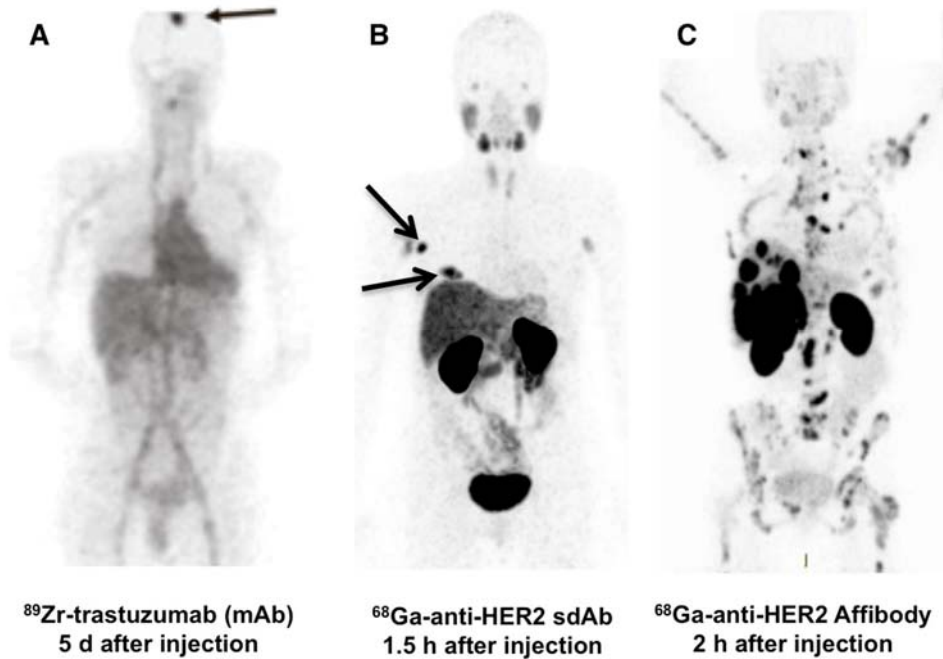


**Figure 1.** Maximum Intensity Projection PET images from patients with metastatic HER2-positive breast cancer, imaged with the monoclonal antibody Trastuzumab (A), the antibody-derived sdAb (B) or scaffold protein Affibody molecule (C) at time points as indicated below the figures. Arrows indicate tumor lesions in A en B. Images adapted from (7,21,42) and with permission from (42). *HER2: human epidermal growth factor receptor 2; mAb: monoclonal antibody, sdAb: single-domain antibody fragment.*

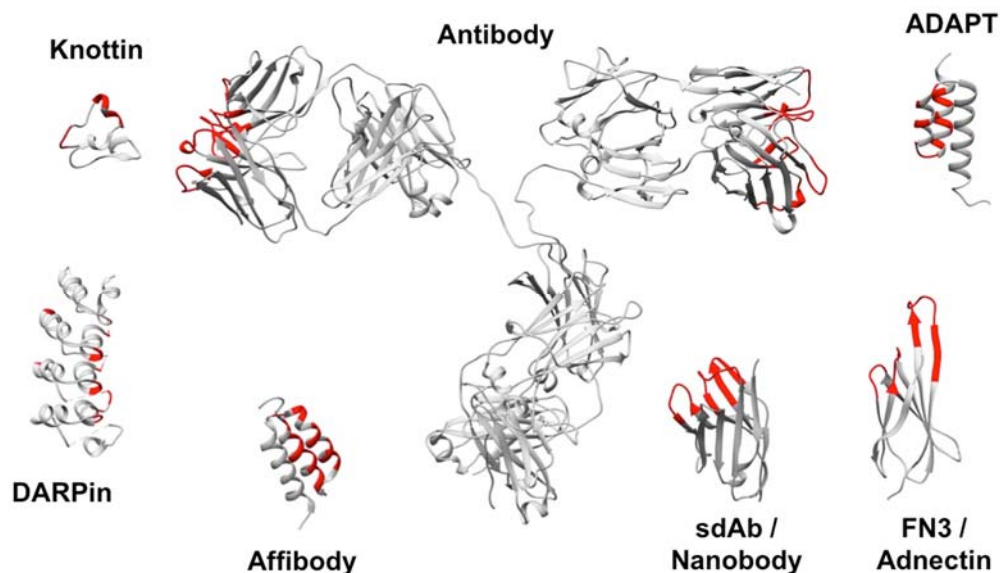


**Figure 2.** Schematic illustration of the structures of the various targeting vehicles discussed in this review. Most-frequent variable stretches and residues are colored red. Note that the structures are sized relative to each other. Representative PDB files were retrieved from the RCSB Protein Data Bank and manipulated using Chimera software: 1IGT (Antibody), 5MY6 (sdAb/Nanobody), 2KZJ (Affibody), 4HRM (DARPin), 2N8B (Knottin), 3QWQ (Adnectin) and 1GJT (ADAPT). *ADAPTs: ABD-derived affinity proteins, DARPins: designed ankyrin repeat proteins, FN3: fibronectin type III, sdAb: single-domain antibody fragments.*

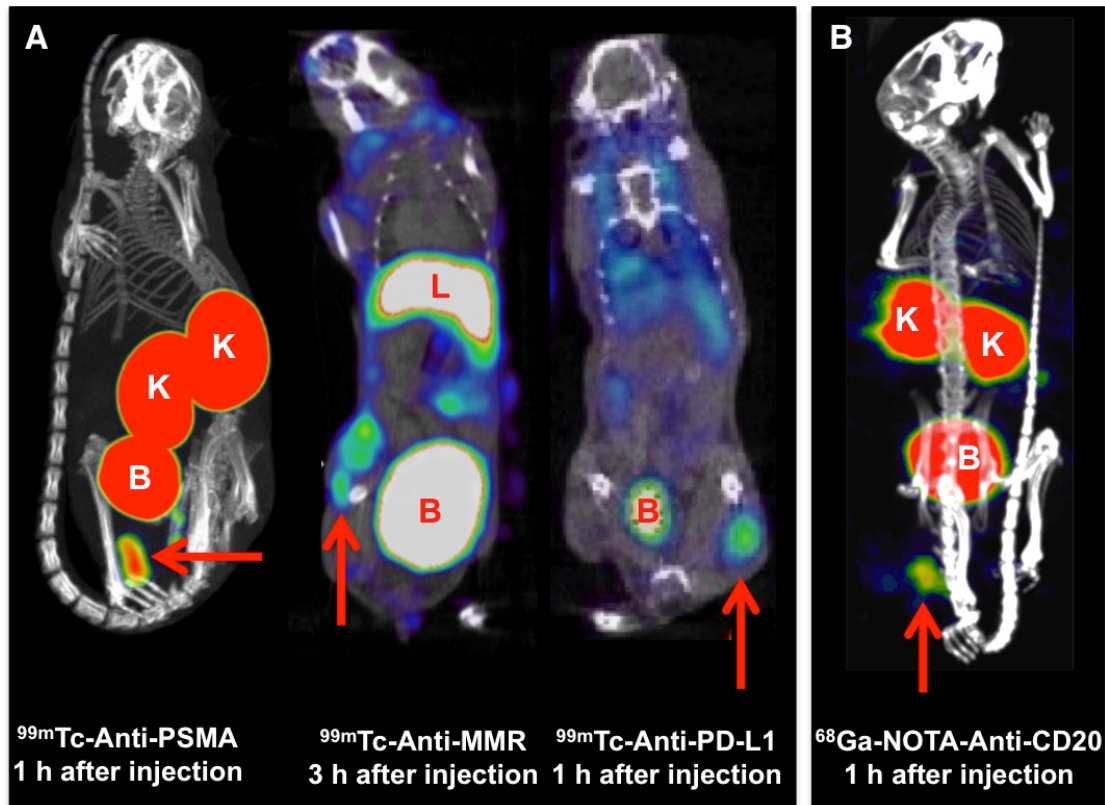


**Figure 3.** SPECT/CT (A) and PET/CT (B) images using sdAb-based tracers in mouse models, showing specific uptake in positive tumor models (arrows). The different targets are stated below each image. Adapted from (13,15,16,18) and with permission from (13). *K: kidney; B: bladder; L: liver; sdAb: single-domain antibody fragments; PSMA: prostate-specific membrane antigen; MMR: macrophage mannose receptor; PD-L1: programmed death-ligand 1.*



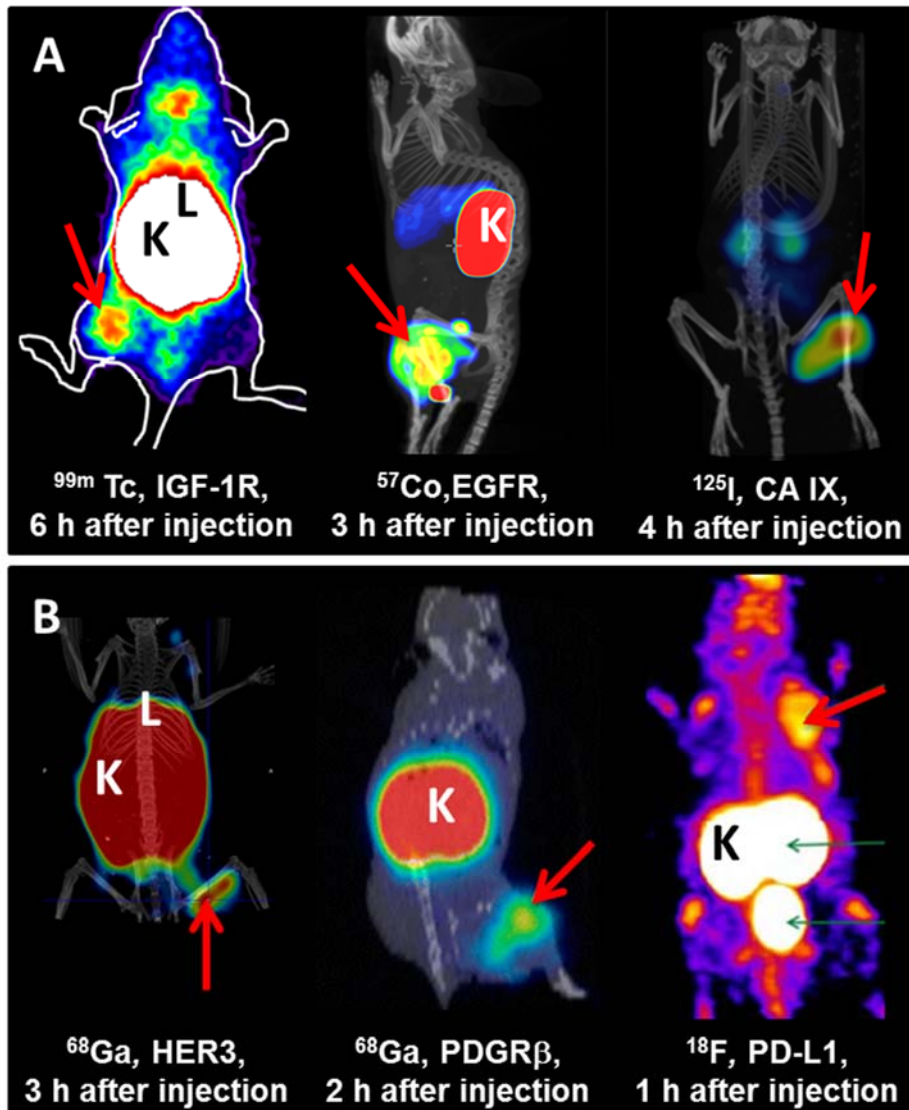


**Figure 4.** Gamma-camera or SPECT/CT (A) and PET/CT (B) imaging using affibody molecules-based tracers in mice, showing uptake in positive tumor models (red arrows). The targets are stated below each image. Adapted from (28-32,43) and with permission from (28,30,31). IGF-1R: *insulin-like growth factor type 1 receptor*; EGFR: *epidermal growth factor receptor*; CAIX: *carbonic anhydrase IX*; HER3: *human epidermal growth factor type 3*; PDGFR $\beta$ : *platelet-derived growth factor receptor beta*; PD-L1: *programmed death-ligand*. K: kidney; L: liver.

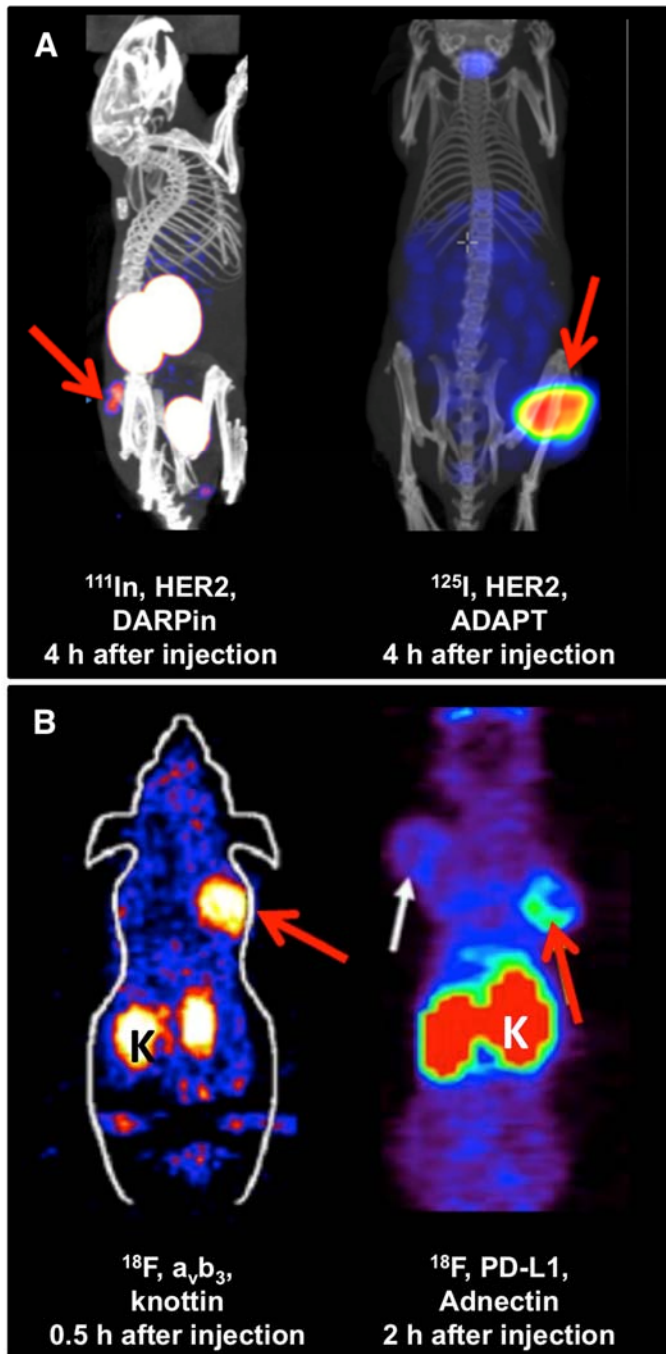


**Figure 5.** SPECT/CT (A) and PET/CT (B) imaging using engineered scaffold protein-based tracers in mice, showing uptake in positive tumor models (red arrows). The types of tracers and targets are stated below each image. Adapted from (35,36,38,40). *DARPin*s: designed ankyrin repeat proteins, *ADAPT*s: ABD-derived affinity proteins, *PD-L1*: programmed death-ligand. *K*: kidney.

**Table 1. Overview of radioactively labeled targeting proteins that have been used *in vivo* for same-day imaging in the last 5 years**

Type	Parent Protein	Target	Compound name	Radio-nuclide	Stage of development	Tumor-to-blood ratio (time post injection)	References
ADAPT	Albumin-binding domain of streptococcal protein G	HER2	C-(HE) <sub>3</sub> -ADAPT6	<sup>68</sup> Ga	Preclinical	17±2 (1h)	(39)
			C-(HE) <sub>3</sub> -ADAPT6	<sup>111</sup> In	Preclinical	43±11 (1h)	(39)
			Cys <sup>59</sup> -(HE)3DANS-ADAPT6	<sup>111</sup> In	Preclinical	277±35 (4h)	(40)
			Cys <sup>59</sup> -(HE)3DANS-ADAPT6	<sup>125</sup> I	Preclinical	53±10 (4h)	(40)
			Cys <sup>2</sup> -(HE)3DANS-ADAPT6	<sup>111</sup> In	Preclinical	254±37 (4h)	(40)
			Cys <sup>2</sup> -(HE)3DANS-ADAPT6	<sup>125</sup> I	Preclinical	61±14 (4h)	(40)
Adnectin	10th domain of human Fibronectin (Type III)	CD20	FN3 <sub>CD20</sub>	<sup>64</sup> Cu	Preclinical	4 (24h )	(37)
		PD-L1	BMS-986192	<sup>18</sup> F	Preclinical	~2 (2h)	(38)
Affibody molecule	Z-domain of staphylococcal protein A	HER2	ABY-025	<sup>68</sup> Ga	Clinical	ND	(21)
				<sup>111</sup> In	Clinical	ND	(20)
			ZHER2:V2	<sup>188</sup> Re	Preclinical	160 (8h)	(24)
		HER3	Z08698	<sup>111</sup> In	Preclinical	12±3 (4h)	(29)
			Z08699	<sup>68</sup> Ga	Preclinical	25±6 (3h)	(29)
		IGF-1R	ZIGF1R:4551	<sup>99m</sup> Tc	Preclinical	7±3 (4h)	(29)
		EGFR	ZEGFR:2377	<sup>99m</sup> Tc	Preclinical	4.4±0.3 (8 h)	(28)
		CAIX	ZCAIX:2	<sup>68</sup> Ga	Preclinical	7±2 (3h)	(43)
			ZCAIX:4	<sup>57/55</sup> Co	Preclinical	12±2 (3h)	(43)
			ZCAIX:4	<sup>99m</sup> Tc	Preclinical	44±7 (4h)	(30)
PDGFRβ	Z09591	<sup>125</sup> I	Preclinical	23±3 (4h)	(30)		
PD-L1	Z <sub>PD-L1_1</sub>	<sup>68</sup> Ga	Preclinical	8±3 (2h)	(31)		
DARPin	Natural Ankyrin Repeat Domains	HER2	G3	<sup>18</sup> F	Preclinical	5.3 (1.5h)	(32)
			G3	<sup>125</sup> I	Preclinical	4±3 (4h)	(36)
Knottin	Inhibitor cystine-knots	α <sub>v</sub> β <sub>6</sub>	S <sub>0</sub> 2	<sup>111</sup> In	Preclinical	174±26 (4h)	(36)
			7c	<sup>64</sup> Cu	Preclinical	10±6 (1h)	(33)
			3-4A	<sup>111</sup> In	Preclinical	9±3 (0.5h)	(34)
sdAbs, Nanobody	Heavy-chain-only antibodies	HER2	2Rs15d	<sup>18</sup> F	Preclinical	6±1 (0.5h)	(35)
			2Rs15d	<sup>68</sup> Ga	Preclinical	13±2 (1h)	(8)
			2Rs15d	<sup>68</sup> Ga	Preclinical	14±3 (1h)	(6)
			2Rs15d	Clinical	ND	(7)	
		<sup>131</sup> I	Preclinical	~25 (1h)	(9)		

	5F7	<sup>18</sup> F	Preclinical	47±13 (2h)	(10)
	5F7GGC	<sup>131</sup> I	Preclinical	11±2 (1h)	(12)
MMR	3.49	<sup>18</sup> F	Preclinical	~2 (3h)	(17)
	cl1	<sup>99m</sup> Tc	Preclinical	20-30 (3h)	(16)
CD20	9079	<sup>68</sup> Ga	Preclinical	~4 (1.5h)	(15)
PSMA	JVZ-007	<sup>111</sup> In	Preclinical	48±5 (3h)	(14)
	PSMA30	<sup>99m</sup> Tc	Preclinical	9±1 (1.5h)	(13)
PD-L1	C3	<sup>99m</sup> Tc	Preclinical	~7 (1.5h)	(18)
	E2	<sup>99m</sup> Tc	Preclinical	~8 (1.5h)	(18)

*ADAPTs: ABD-derived affinity proteins; CAIX: carbonic anhydrase IX; DARPins: designed ankyrin repeat proteins; EGFR: Epidermal growth factor receptor; HER2: human epidermal growth factor type 2; IGF-1R: insulin-like growth factor type 1 receptor; MMR: macrophage mannose receptor; ND: not determined; PDGFR $\beta$ : platelet-derived growth factor receptor beta; ; PD-L1: programmed death-ligand 1; PSMA: prostate-specific membrane antigen; sdAb: single-domain antibody fragment.*